

## Transcription factor organic cation transporter 1 (OCT-1) affects the expression of porcine Klotho (KL) gene

Yan Li, Lei Wang, Jiawei Zhou, Fenge Li

Klotho (KL), originally discovered as an aging suppressor, was a membrane protein that shared sequence similarity with the  $\beta$ -glucosidase enzymes. Recent reports showed Klotho might have a role in adipocyte maturation and systemic glucose metabolism. However, little is known about the transcription factors involved in regulating the expression of porcine *KL* gene. Deletion fragment analysis identified KL-D2 (-418 bp to -3 bp) as the porcine *KL* core promoter. MARC0022311 in *KL* intron 1 appeared a polymorphism (A or G) in Landrace  $\times$  DIV pigs, and relative luciferase activity of *pGL3-D2-G* was significantly higher than *pGL3-D2-A*. This was possibly the result of a change in *KL* binding ability with transcription factor organic cation transporter 1 (OCT-1), which was confirmed using electrophoretic mobility shift assays (EMSA) and chromatin immunoprecipitation (ChIP). Moreover, OCT-1 regulated endogenous *KL* expression by RNA interference. Our study indicates SNP MARC0022311 affects porcine *KL* expression by regulating its promoter activity via OCT-1.



**12 Abstract**

13 Klotho (KL), originally discovered as an aging suppressor, was a membrane protein that shared  
14 sequence similarity with the  $\beta$ -glucosidase enzymes. Recent reports showed Klotho might have a  
15 role in adipocyte maturation and systemic glucose metabolism. However, little is known about  
16 the transcription factors involved in regulating the expression of porcine *KL* gene. Deletion  
17 fragment analysis identified KL-D2 (-418 bp to -3 bp) as the porcine *KL* core promoter.  
18 MARC0022311 in *KL* intron 1 appeared a polymorphism (A or G) in Landrace $\times$  DIV pigs, and  
19 relative luciferase activity of *pGL3-D2-G* was significantly higher than *pGL3-D2-A*. This was  
20 possibly the result of a change in *KL* binding ability with transcription factor organic cation  
21 transporter 1 (OCT-1), which was confirmed using electrophoretic mobility shift assays (EMSA)  
22 and chromatin immunoprecipitation (ChIP). Moreover, OCT-1 regulated endogenous *KL*  
23 expression by RNA interference. Our study indicates SNP MARC0022311 affects porcine *KL*  
24 expression by regulating its promoter activity via OCT-1.

**25 Keywords**

26 Pig; *KL* gene; OCT-1; MARC0022311

## 27 **Introduction**

28 Klotho (*KL*) gene encoded a membrane protein that shared sequence similarity with the  $\beta$ -  
29 glucosidase enzymes and its product might function as part of a signaling pathway that regulated  
30 aging *in vivo* and morbidity in age-related diseases (Ko et al., 2013). Mutant mice lacking the *KL*  
31 gene showed multiple aging disorders and a shortened life span (Kuro-o et al., 1997). *KL/KL*  
32 mice had the pattern of ectopic calcification certainly contributed by the elevated phosphate and  
33 calcium levels (Hu et al., 2011; Ohnishi et al., 2009). *KL* also acted as a deregulated factor of  
34 mineral metabolism in autosomal dominant polycystic kidney disease (Mekahli & Bacchetta.,  
35 2013). Mice that lacked Klotho activity were lean owing to reduced white adipose tissue  
36 accumulation, and were resistant to obesity induced by a high-fat diet (Ohnishi et al., 2011;  
37 Razzaque et al., 2012).

38 *KL* expression is regulated by thyroid hormone, oxidative stress, long-term hypertension and so  
39 on (Koh et al., 2001). Some transcription factors such as peroxisome proliferator-activated  
40 receptor gamma (PPAR- $\gamma$ ) also could regulate *KL* expression (Zhang et al., 2008). A double-  
41 positive feedback loop between PPAR- $\gamma$  and Klotho regulated adipocyte maturation (Chihara et  
42 al., 2006; Zhang et al., 2008). Briefly, chromatin immuno-precipitation (ChIP) and gel shift  
43 assays found a PPAR-responsive element within the 5'-flanking region of human *KL* gene.  
44 Additionally, PPAR- $\gamma$  agonists increased *KL* expression in HEK293 cells and several renal  
45 epithelial cell lines, while the induction was blocked by PPAR- $\gamma$  antagonists or small interfering  
46 RNAs (Zhang et al., 2008). Furthermore, Klotho could induce PPAR- $\gamma$  synthesis during  
47 adipocyte maturation (Chihara et al., 2006). However, little is known about the transcription

48 factors involved in regulating the expression of porcine *KL* gene.

49 To investigate the transcriptional regulation of porcine *KL* gene, we identified the core promoter  
50 of porcine *KL* gene, analyzed its upstream regulatory elements and revealed that transcription  
51 factor OCT1 directly bound to the core promoter region of porcine *KL* gene and regulated its  
52 expression.

### 53 **Materials and Methods**

#### 54 **Ethics statements**

55 All animal procedures were performed according to protocols approved by the Biological Studies  
56 Animal Care and Use Committee of Hubei Province, PR China. Sample collection was approved  
57 by the ethics committee of Huazhong Agricultural University (No. 30700571 for this study).

#### 58 **MARC0022311 polymorphism in pigs**

59 Nineteen Landrace × DIV crossbred pigs were genotyped with the Porcine SNP60 BeadChip  
60 (Illumina) using the Infinium HD Assay Ultra protocol, which was conducted under the technical  
61 assistance by Compass Biotechnology Corporation. DIV was a synthetic line derived by crossing  
62 Landrace, Large White, Tongcheng or Meishan pigs. Raw data had high genotyping quality (call  
63 rate > 0.99) and were analyzed with the GenomeStudio software.

#### 64 ***In silico* sequence analysis**

65 *KL* gene sequence ENSSSCG00000009347 was available on the ENSEMBL online website  
66 (<http://asia.ensembl.org/index.html>). We obtained the up-stream sequence for *KL* promoter  
67 prediction. The potential promoter was analyzed using the online neural network promoter  
68 prediction (NNPP) ([http://www.fruitfly.org/seq\\_tools/promoter.html](http://www.fruitfly.org/seq_tools/promoter.html)) and Promoter 2.0 prediction

69 server (<http://www.cbs.dtu.dk/services/Promoter/>). Transcription factor binding sites were  
70 predicted using biological databases (BIOBASE) (<http://www.gene-regulation.com/pub/programs.html>) with a threshold of 0.90 and TFsearch (<http://www.cbrc.jp/research/db/TFSEARCH.html>) with a threshold of 85.

### 73 **Cell culture, transient transfection and luciferase assay**

74 The porcine kidney (PK) cells and swine testis (ST) cells obtained from China Center for Type  
75 Culture Collection (CCTCC) were cultured at 37 °C in a humidified atmosphere of 5% CO<sub>2</sub>  
76 using DMEM supplemented with 10% FBS (Gibco).

77 Four *KL* promoter deletion fragments were cloned into *pGL3-Basic* vector to determine the core  
78 promoter region. The plasmids contained pig *KL-D2* promoter and *KL* intron 1 fragments  
79 (g.1474 A and g.1474 G) were reconstructed, then transfected using lipofectamine 2000  
80 (Invitrogen) into PK cells and ST cells. Plasmid DNA of each well used in the transfection  
81 containing 0.8 µg of *KL* promoter constructs and 0.04 µg of the internal control vector *pRL-TK*  
82 Renilla/luciferase plasmid. The enzymatic activity of luciferase was then measured with  
83 PerkinElmer 2030 Multilabel Reader (PerkinElmer).

### 84 **RNA interference**

85 Double-stranded small interfering RNAs (siRNAs) targeting *OCT-1* were obtained from  
86 GenePharma. Cells were co-transfected with 2 µl of siRNA, 0.2 µg of reconstructed plasmids  
87 using Lipofetamine 2000™ reagent for 24 h. Transfection mixtures were removed, and fresh  
88 complete DMEM medium was added to each well. Finally, the enzymatic activity of luciferase  
89 was then measured with PerkinElmer 2030 Multilabel Reader (PerkinElmer).

## 90 **Quantitative real time PCR (qPCR)**

91 qPCR was performed on the LightCycler® 480 (Roche) using SYBR® Green Real-time PCR  
92 Master Mix (Toyobo). Primers used in the qPCR were shown in Table 1. qPCR conditions  
93 consisted of 1 cycle at 94 °C for 3 min, followed by 40 cycles at 94 °C for 40 sec, 61 °C for 40 sec,  
94 and 72 °C for 20 sec, with fluorescence acquisition at 74 °C. All PCRs were performed in  
95 triplicate and gene expression levels were quantified relatively to the expression of  $\beta$ -actin.  
96 Analysis of expression level was performed using the  $2^{-\Delta\Delta C_t}$  method (Livak & Schmittgen, 2001).  
97 Student's t-test was used for statistical comparisons.

## 98 **Western blotting**

99 Western blotting was performed as described previously (Tao et al., 2014). Five  $\mu$ g proteins were  
100 boiled in  $5 \times$  SDS buffer for 5 min, separated by SDS-PAGE, and transferred to PVDF  
101 membranes (Millipore). Then, the membranes were blocked with skim milk and probed with  
102 anti-KL (ABclonal).  $\beta$ -actin (Santa Cruz) was used as a loading control. The results were  
103 visualized with horseradish peroxidase-conjugated secondary antibodies (Santa Cruz) and  
104 enhanced chemiluminescence.

## 105 **Electrophoretic mobility shift assays (EMSA)**

106 Nuclear protein of PK and ST cells was extracted with Nucleoprotein Extraction Kit (Beyotime).  
107 The oligonucleotides (Sangon) corresponding to the OCT-1 binding sites of *KL* intron 1 (Table 1)  
108 were synthesized and annealed into double strands. The DNA binding activity of OCT-1 protein  
109 was detected by LightShift® Chemiluminescent EMSA Kit (Pierce). Ten  $\mu$ g nuclear extract was  
110 added to 20 fmol biotin-labeled double stranded oligonucleotides, 0.1 mM EDTA, 2.5% Glycerol,

111 1×binding buffer, 5 mM MgCl<sub>2</sub>, 50 ng Poly (dI·dC) and 0.05% NP-40. In addition, control group  
112 added 2 pmol unlabeled competitor oligonucleotides, while the super-shift group added 10 µg  
113 OCT-1 antibodies (Santa Cruz). The mixtures were then incubated at 24 °C for 20 min. The  
114 reactions were analyzed by electrophoresis in 5.5% polyacrylamide gels at 180 V for 1 h, and  
115 then transferred to a nylon membrane. The dried nylon was scanned with GE ImageQuant  
116 LAS4000 mini (GE-Healthcare).

### 117 **Chromatin immunoprecipitation (ChIP) assay**

118 ChIP assays were performed using a commercially available ChIP Assay Kit (Beyotime) as  
119 previously described (Tao et al., 2015). Briefly, after crosslinking the chromatin with 1%  
120 formaldehyde at 37 °C for 10 min and neutralizing with glycine for 5 min at room temperature,  
121 PK and ST cells were washed with cold PBS, scraped and collected on ice. Then, cells were  
122 harvested, lysed and treated by sonication. Nuclear lysates were processed 20 times for 10 sec  
123 with 20 min intervals on ice water using a Scientz-IID (Scientz). An equal amount of chromatin  
124 was immune-precipitated at 4 °C overnight with at least 1.5 µg of OCT-1 antibody (Santa Cruz)  
125 and normal mouse IgG antibody (Millipore). Immune-precipitated products were collected after  
126 incubation with Protein A + G coated magnetic beads. The beads were washed, and the bound  
127 chromatin was eluted in ChIP elution buffer. Then the proteins were digested with Proteinase K  
128 for 4 h at 45 °C. The DNA was purified using the AxyPrep PCR Cleanup Kit (Axygen). The  
129 DNA fragment of OCT-1 binding sites in *KL* intron 1 was amplified with the specific primers  
130 (Table 1).

### 131 **Results**

**132 MARC0022311 status in pigs**

133 MARC0022311 in *KL* intron 1 appeared a polymorphism (A or G) in 19 Landrace× DIV pigs,  
134 with 12 AA pigs and AG pigs genotyped using the Illumina PorcineSNP60 chip (Supplementary  
135 dataset). The SNP (MARC0022311) in pig *KL* intron 1 was renamed as *KL* g.1474 A>G  
136 according to the standard mutation nomenclature (den Dunnen & Antonarakis, 2000).

**137 Identification of promoter region of the porcine *KL* gene**

138 An 833 bp contig in 5' flanking region of pig *KL* gene was obtained by PCR. To determine the  
139 promoter region, four promoter deletions (KL-D1: -178 bp to -3 bp, KL-D2: -418 bp to -3 bp,  
140 KL-D3: -599 bp to -3 bp and KL-D4: -835 bp to -3 bp) were cloned into fluorescent vector based  
141 on the prediction of NNPP online software and Promoter 2.0 (Fig. 1A). Luciferase activity  
142 analysis in both PK and ST cells revealed that KL-D2 (-418 bp to -3 bp) was essential for its  
143 transcriptional activity and was defined as the *KL* promoter region (Fig. 1B).

**144 MARC0022311 SNP affects the *KL* expression**

145 Intron SNPs could not change the amino acid sequence, but might alter gene promoter activity by  
146 affecting the binding of transcription factors (Van Laere et al., 2003). The plasmids contained  
147 KL-D2 and the wild-type A (g.1474 A) or mutant G (g.1474 G) sequence were named as *pGL3-*  
148 *D2-A* and *pGL3-D2-G*, respectively. Results showed that luciferase activity of *pGL3-D2-G* was  
149 significantly higher than *pGL3-D2-A* in both PK cells ( $P < 0.05$ ) and ST cells ( $P < 0.01$ ) (Fig.  
150 2A), indicating the binding of certain regulatory elements affected *KL* promoter activity.

151 The SNP (MARC0022311) located in the first intron of *KL* gene (+1474 bp) was predicted to  
152 change the binding of OCT-1 by BIOBASE and TFsearch (Fig. S1). siRNAs were used to knock

153 down *OCT-1* in PK and ST cells. After silencing *OCT-1*, luciferase activity of *pGL3-D2-G* was  
154 significantly lower than *pGL3-D2-A* in both PK cells and ST cells ( $P < 0.05$ ) (Figs. 2B and 2C).  
155 Furthermore, compared with the negative control, the luciferase activity of *pGL3-D2-A* was  
156 significantly decreased ( $P < 0.05$ ) (Figs. 2B and 2C). Thus, MARC0022311 regulated the  
157 promoter activity via OCT-1.

158 However, inhibition of *OCT-1* expression significantly suppressed *KL* expression in PK and ST  
159 cells ( $P < 0.05$ ) (Fig. 3), possibly because OCT-1 could stimulate *KL* expression by binding *KL*  
160 gene at other sites.

#### 161 **Transcription factor OCT-1 binds to the *KL* intron 1 both *in vitro* and *in vivo***

162 To address whether *KL* intron 1 contained OCT-1 binding sites *in vitro*, we used two  
163 oligonucleotides (A allele and G allele oligonucleotides) with differing only at SNP  
164 MARC0022311 position, as porcine OCT-1 probes in EMSA. EMSA revealed a highly specific  
165 interaction with allele A oligonucleotide, and a 100 fold excess of mutant allele G  
166 oligonucleotide could not outcompete the interaction (Fig. 4A). A super-shift was obtained when  
167 nuclear extracts from PK and ST cells were incubated with OCT-1 antibodies, providing further  
168 biochemical evidence for the presence of OCT-1 *in vitro* (Fig. 4A). We found the *KL* genotype at  
169 g.1474 A>G locus was AA in PK and ST cells by PCR-sequencing, indicating the endogenous  
170 binding of OCT-1 to *KL* in above two cell lines (Fig. S2). The chromatin was immune-  
171 precipitated using an OCT-1 antibody and DNA fragments of the expected size were used as a  
172 template to perform PCR amplification. ChIP analysis showed that OCT-1 interacted with *KL*  
173 intron 1 (Fig. 4B). These results showed that transcription factor OCT-1 bound to *KL* intron 1

174 both *in vitro* and *in vivo*.

## 175 **Discussion**

176 *KL* gene encodes a type-I membrane protein that is related to beta-glucosidases (Ko et al., 2013).

177 *KL* might function as part of a signaling pathway that regulated morbidity in age-related diseases

178 such as atherosclerosis and cardiovascular disease, and mineral metabolism diseases such as

179 ectopic calcification (Ko et al., 2013; Kuro-o et al., 1997; Hu et al., 2011; Ohnishi et al., 2009).

180 Overexpression of *KL* in the preadipocyte 3T3-L1 cell line can induce expression of several

181 adipogenic markers, including *PPAR $\gamma$* , CCAAT/enhancer binding protein alpha (*C/EBP $\alpha$* ) and

182 CCAAT/enhancer binding protein delta (*C/EBP $\delta$* ), and facilitate the differentiation of

183 preadipocytes into mature adipocytes (Chihara et al., 2006). Eliminating *KL* function from mice

184 resulted in the generation of lean mice with almost no detectable fat tissue, and induced a

185 resistance to high-fat-diet-stimulated obesity (Razzaque et al., 2012; Ohnishi et al., 2011).

186 Here we found the SNP MARC0022311 located in *KL* intron 1 showed a polymorphism in the

187 tested pigs (Supplementary dataset). A number of SNPs were proved to have major effects on the

188 phenotypic variations (Markljung et al., 2009; Milan et al., 2000; Ren et al., 2011; Van Laere et

189 al., 2003). Previous research reported that a G to A transition in intron 3 of porcine insulin-like

190 growth factor 2 (*IGF2*) affected the binding of ZBED6 and significantly up-regulated *IGF2*

191 expression in skeletal muscle (Markljung et al., 2009; Van Laere et al., 2003). We predicted the

192 SNP MARC0022311 located in *KL* intron 1 could change the binding of transcription factors

193 including OCT1 by BIOBASE and TFsearch online software (Fig. S1).

194 The Octamer-binding proteins (OCTs) are a group of highly conserved transcription factors that

195 specifically bind to the octamer motif (ATGCAAAT) and closely related sequences that are  
196 found in promoters and enhancers (Zhao, 2013). OCT1 regulates the expression of a variety of  
197 genes, including immunoglobulin genes (Dreyfus, Doyen & Rougeon, 1987),  $\beta$ -casein gene  
198 (Zhao, Adachi & Oka, 2002), miR-451/ AMPK signaling (Ansari et al., 2015), sex-determining  
199 region Y gene (Margarit et al., 1998), synbindin – related ERK signaling (Qian et al., 2015).

200 In the present study, luciferase activity of *pGL3-D2-G* was significantly higher than *pGL3-D2-A*  
201 in PK cells and ST cells and the following *OCT-1* RNAi results showed that luciferase activity of  
202 *pGL3-D2-G* significantly decreased, confirming OCT-1 was the repressor. Therefore, we  
203 supposed that OCT-1 could bind to the first intron of *KL* when the SNP was allele A, and then  
204 depressed activity of *KL* promoter.

205 However, the expression of *KL* was significantly inhibited after silencing *OCT-1*. There were  
206 several OCT-1 binding sites in porcine *KL* gene. One hundred and sixty six OCT-1 binding sites  
207 were predicted in intron 1 (36324 bp in length) by BIOBASE and TFsearch online software (Fig.  
208 S3A). ChIP analysis showed that OCT-1 interacted with all of three tested regions (1395 bp to  
209 1525 bp, 14322 bp to 14436 bp, 30970 bp to 31141 bp) in PK cells (Fig. S3B). In consequence,  
210 we hypothesized that OCT-1 could bind *KL* gene at multiple sites, and the positive regulation of  
211 *KL* gene might be dominant.

212 Klotho physiologically regulate mineral and energy metabolism by influencing the activities of  
213 fibroblast growth factors (FGFs) including FGF-2, FGF-19, FGF-23 and their receptors (FGFRs)  
214 (Guan et al., 2014; Razzaque et al., 2009; Wu et al., 2008). Taken together, *KL* exerts its function  
215 via OCT-1 - *KL*- FGF- FGFR pathway.

## 216 **Conclusions**

217 In summary, SNP MARC0022311 affected OCT-1 binding ability with the *KL* promoter. And  
218 the *KL* promoter activity was significantly decreased with allele A of MARC0022311 compared  
219 with allele G. Our study indicates SNP MARC0022311 affects porcine *KL* expression by  
220 regulating its promoter activity via OCT-1.

## 221 **Acknowledgements**

222 We are grateful to Compass Biotechnology Corporation for technical assistance with Illumina  
223 SNP analysis. The authors also acknowledge the farmers for providing pig samples.

## 224 **References**

- 225 Ansari KI, Ogawa D, Rooj AK, Lawler SE, Krichevsky AM, Johnson MD, Chiocca EA,  
226 Bronisz A, Godlewski J. 2015. Glucose-based regulation of miR-451/AMPK signaling  
227 depends on the OCT1 transcription factor. *Cell Reports* 11(6):902-909 DOI  
228 10.1016/j.celrep.2015.04.016.
- 229 Chihara Y, Rakugi H, Ishikawa K, Ikushima M, Maekawa Y, Ohta J, Kida I, Ogihara T. 2006.  
230 Klotho protein promotes adipocyte differentiation. *Endocrinology* 147(8):3835-3842 DOI  
231 10.1210/en.2005-1529.
- 232 Den Dunnen JT, Antonarakis SE. 2000. Mutation nomenclature extensions and suggestions to  
233 describe complex mutations: a discussion. *Human Mutation* 15:7-12  
234 DOI 10.1002/(SICI)1098-1004(200001)15:1<7::AID-HUMU4>3.0.CO;2-N.
- 235 Dreyfus M, Doyen N, Rougeon F. 1987. The conserved decanucleotide from the

236 immunoglobulin heavy chain promoter induces a very high transcriptional activity in B-  
237 cells when introduced into a heterologous promoter. *EMBO Journal* 6:1685-1690.

238 Guan X, Nie L, He T, Yang K, Xiao T, Wang S, Huang Y, Zhang J, Wang J, Sharma K, Liu  
239 Y, Zhao J. 2014. Klotho suppresses renal tubulo- interstitial fibrosis by controlling  
240 basic fibroblast growth factor-2 signalling. *The Journal of Pathology* 234(4):560-572 DOI  
241 10.1002/path.4420.

242 Hu MC, Shi M, Zhang J, Quiñones H, Griffith C, Kuro-o M, Moe OW. 2011.  
243 Klotho deficiency causes vascular calcification in chronic kidney disease. *Journal of the*  
244 *American Society of Nephrology* 22(1):124-136 DOI 10.1681/ASN.2009.

245 Ko GJ, Lee YM, Lee EA, Lee JE, Bae SY, Park SW, Park MS, Pyo HJ, Kwon YJ, WDPA.  
246 2013. The association of Klotho gene polymorphism with the mortality of patients on  
247 maintenance dialysis. *Clinical Nephrology* 80(4):263-269 DOI 10.5414/CN107800.

248 Koh N, Fujimori T, Nishiguchi S, Tamori A, Shiomi S, Nakatani T, Sugimura K, Kishimoto  
249 T, Kinoshita S, Kuroki T, Nabeshima Y. 2001. Severely reduced production of Klotho in  
250 human chronic renal failure kidney. *Biochemical and Biophysical Research*  
251 *Communications* 280:1015-1020 DOI 10.1006/bbrc.2000.4226.

252 Kuro-o M, Matsumura Y, Aizawa H, Kawaguchi H, Suga T, Utsugi T, Ohyama Y, Kurabayashi  
253 M, Kaname T, Kume E, Iwasaki H, Iida A, Shiraki-Iida T, Nishikawa S, Nagai R,  
254 Nabeshima YI. 1997. Mutation of the mouse klotho gene leads to a syndrome resembling  
255 ageing. *Nature* 390(6655):45-51 DOI 10.1038/36285.

256 Livak KJ, Schmittgen TD. 2001. Analysis of relative gene expression data using real-time

- 257 quantitative PCR and the 2(-Delta Delta C(T)) Method. *Methods* 25(4):402-408 DOI  
258 10.1006/meth.2001.1262.
- 259 Markljung E, Jiang L, Jaffe JD, Mikkelsen TS, Wallerman O, Larhammar M, Zhang X, Wang  
260 L, Saenz-Vash V, Gnirke A, Lindroth AM, Barrés R, Yan J, Strömberg S, De S, Pontén  
261 F, Lander ES, Carr SA, Zierath JR, Kullander K, Wadelius C, Lindblad-Toh K, Andersson  
262 G, Hjältn G, Andersson L. 2009. ZBED6, a novel transcription factor derived from a  
263 domesticated DNA transposon regulates IGF2 expression and muscle growth.  
264 *PLOS Biology* 7(12): e1000256 DOI 10.1371/journal.pbio.1000256.
- 265 Margarit E, Guillén A, Rebordosa C, Vidal-Taboada J, Sánchez M, Ballesta F, Oliva R. 1998.  
266 Identification of conserved potentially regulatory sequences of the SRY gene from 10  
267 different species of mammals. *Biochemical and Biophysical Research Communications*  
268 245(2): 370-377 DOI 10.1006/bbrc.1998.8441.
- 269 Mekahli D, Bacchetta J. 2013. From bone abnormalities to mineral metabolism dysregulation in  
270 autosomal dominant polycystic kidney disease. *Pediatric Nephrology* 28:2089-2096 DOI  
271 10.1007/s00467-012-2384-5.
- 272 Milan D, Jeon JT, Looft C, Amarger V, Robic A, Thelander M, Rogel-Gaillard C, Paul  
273 S, Iannuccelli N, Rask L, Ronne H, Lundström K, Reinsch N, Gellin J, Kalm E, Roy  
274 PL, Chardon P, Andersson L. 2000. A mutation in PRKAG3 associated with excess  
275 glycogen content in pig skeletal muscle. *Science* 288(5469):1248-51.

- 276 Ohnishi M, Kato S, Akiyoshi J, Atfi A, Razzaque MS. 2011. Dietary and genetic evidence for  
277 enhancing glucose metabolism and reducing obesity by inhibiting klotho functions.  
278 The FASEB Journal 25(6): 2031-2039 DOI 10.1096/fj.10-167056.
- 279 Ohnishi M, Nakatani T, Lanske B, Razzaque MS. 2009. Reversal of mineral ion homeostasis and  
280 soft-tissue calcification of klotho knockout mice by deletion of vitamin D 1alpha-  
281 hydroxylase. Kidney International 75:1166-1172 DOI 10.1038/ki.2009.24.
- 282 Qian J, Kong X, Deng N, Tan P, Chen H, Wang J, Li Z, Hu Y, Zou W, Xu J, Fang JY. 2015.  
283 OCT1 is a determinant of synbindin-related ERK signalling with independent prognostic  
284 significance in gastric cancer. Gut 64(1):37-48 DOI 10.1136/gutjnl-2013-306584.
- 285 Razzaque MS. 2009. The FGF23-Klotho axis: endocrine regulation of phosphate homeostasis.  
286 Nature Reviews Endocrinology 5(11): 611-619 DOI 10.1038/nrendo.2009.196.
- 287 Razzaque MS. 2012. The role of Klotho in energy metabolism. Nature Reviews Endocrinology  
288 8(10):579-587 DOI 10.1038/nrendo.2012.75.
- 289 Ren J, Duan Y, Qiao R, Yao F, Zhang Z, Yang B, Guo Y, Xiao S, Wei R, Ouyang Z, Ding N, Ai  
290 H, Huang L. 2011. A missense mutation in PPAR $\delta$  causes a major QTL effect on ear size in  
291 pigs. PLoS Genetics 7(5):e1002043 DOI 10.1371/journal.pgen.1002043.
- 292 Tao H, Mei S, Zhang X, Peng X, Yang J, Zhu L, Zhou J, Wu H, Wang L, Hua L, Li F. 2014.  
293 Transcription factor C/EBP $\beta$  and 17 $\beta$ -Estradiol promote transcription of the porcine p53  
294 gene. The International Journal of Biochemistry & Cell Biology 47:76-82 DOI  
295 10.1016/j.biocel.2013.12.002.
- 296 Tao H, Wang L, Zhou J, Pang P, Cai S, Li J, Mei S, Li F. 2015. The transcription factor

297 ccaat/enhancer binding protein  $\beta$  (C/EBP $\beta$ ) and miR-27a regulate the expression of porcine  
298 Dickkopf2 (DKK2). *Scientific Reports* 5:17972 DOI 10.1038/srep17972.

299 Van Laere AS, Nguyen M, Braunschweig M, Nezer C, Collette C, Moreau L, Archibald  
300 AL, Haley CS, Buys N, Tally M, Andersson G, Georges M, Andersson L. 2003. A  
301 regulatory mutation in IGF2 causes a major QTL effect on muscle growth in the pig.  
302 *Nature* 25 (6960):832-836 DOI 10.1038/nature02064.

303 Wu X, Lemon B, Li X, Gupte J, Weiszmann J, Stevens J, Hawkins N, Shen W, Lindberg R, Chen  
304 JL, Tian H, Li Y. 2008. C-terminal tail of FGF19 determines its specificity toward Klotho  
305 co-receptors. *The Journal of Biological Chemistry* 283(48):33304-33309 DOI  
306 10.1074/jbc.M803319200.

307 Zhang H, Li Y, Fan Y, Wu J, Zhao B, Guan Y, Chien S, Wang N. 2008. Klotho is a target gene of  
308 PPAR-gamma. *Kidney International* 74(6):732-739 DOI 10.1038/ki.2008.244.

309 Zhao FQ. 2013. Octamer-binding transcription factors: genomics and functions. *Frontiers in*  
310 *Bioscience (Landmark Ed)*, 18: 1051-1071.

311 Zhao FQ, Adachi K, Oka T. 2002. Involvement of Oct-1 in transcriptional regulation of beta-  
312 casein gene expression in mouse mammary gland. *Biochimica et Biophysica Acta* 1577: 27-  
313 37 DOI 10.1016/S0167-4781(02)00402-5.

315 **Figure Legends**

316 Fig. 1: Deletion analysis of pig *KL* promoter. (A) Schematic diagram of *KL* promoter ,  
317 MARC0022311 (*KL* g.1474 A>G) and OCT-1 binding site in intron 1. (B) Promoter activities of  
318 a series of deleted constructs determined by luciferase assay. Left panel, relative location of four  
319 deletion fragments. The nucleotides were numbered from the potential transcriptional start site  
320 assigned as +1. Right panel, the relative luciferase activities of four reconstructed vector  
321 contained sequence from KL-D1 to KL-D4. \*\*\*  $P < 0.001$ .

322 Fig. 2: MARC0022311 in pig *KL* intron 1 affected promoter activity in PK and ST cells. (A)  
323 Luciferase assays of reporter constructs using pig KL-D2 promoter and intron 1 fragments  
324 (g.1474 A and g.1474 G). (B) Luciferase detection after co-transfection of *OCT-1* siRNA with  
325 *pGL3-D2-A* and *pGL3-D2-G* in PK cells. (C) Luciferase detection after co-transfection of *OCT-1*  
326 siRNA with *pGL3-D2-A* and *pGL3-D2-G* in ST cells. \*  $P < 0.05$ . \*\*  $P < 0.01$ .

327 Fig. 3: OCT-1 up-regulated *KL* expression by RNAi. (A) PK cells were treated with 2  $\mu$ l *OCT-1*  
328 siRNA and 2  $\mu$ l NC for 24 h. Knockdown of *OCT-1* was confirmed by qPCR. *KL* mRNA and  
329 protein expressions were analyzed by qPCR and Western blotting. (B) ST cells were treated with  
330 2  $\mu$ l *OCT-1* siRNA and 2  $\mu$ l NC for 24 h. Knockdown of *OCT-1* was confirmed by qPCR  
331 analysis. *KL* mRNA and protein expressions were analyzed by qPCR and Western blotting. \*  
332  $P < 0.05$ . \*\*  $P < 0.01$ .

333 Fig. 4: Binding of OCT-1 with *KL* intron 1 was analyzed by EMSA and CHIP. (A) The probe  
334 was incubated with nuclear extract in the absence or presence of 100-fold excess of various  
335 competitor probes (mutant or non-labeled probe) or anti-OCT-1. The specific super-shift (DNA-

336 protein-antibody complex) bands were both observed in PK and ST cells. The sequences of  
337 various probes were demonstrated under the panel. (B) ChIP assay of OCT-1 binding to the *KL*  
338 intron 1 in PK cells and ST cells. The interaction of OCT-1 *in vivo* with *KL* intron region was  
339 determined by chromatin immunoprecipitation analysis. DNA isolated from immune-precipitated  
340 material was amplified by PCR to amplify *KL* fragment. Total chromatin was used as the input.  
341 Normal mouse IgG was used as a negative control.  
342

343 Table 1. Primers and DNA oligos used in this study.

344 **Supplementary files**

345 Fig. S1: Transcription factor binding site prediction of the porcine *KL* intron 1 containing  
346 MARC0022311 (KL g.1474 A>G). Quadrilateral frame indicated the substitutions and extra  
347 binding site of OCT-1. (A) Predicted by BIOBASE online software. (B) Predicted by TFserach  
348 online software.

349 Fig. S2: Genotyping results of MARC0022311. (A) PK cells. (B) ST cells. MARC0022311 was  
350 marked in gray background.

351 Fig. S3. OCT-1 binding sites in the porcine *KL* intron 1. (A) Frequency distribution of the  
352 predicted OCT-1 binding sites. X-axis indicated the length of the porcine *KL* intron 1 in bp. Y-  
353 axis was the frequency of the predicted OCT-1 binding sites. (B) ChIP analysis of three  
354 candidate OCT-1 binding sites (1395 bp to 1525 bp, 14322 bp to 14436 bp, 30970 bp to 31141  
355 bp) in *KL* intron 1 in PK cells. Primers used for ChIP-PCR was shown in Table 1. Input and R  
356 were positive control, while IgG was the negative control.

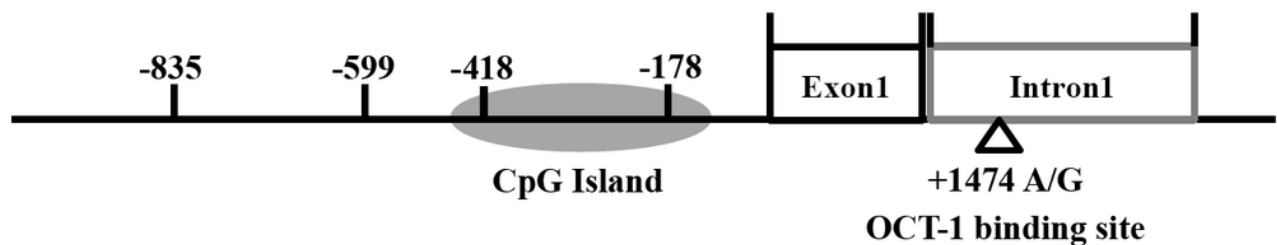
357 Supplementary dataset: SNP genotyping results in 19 Landrace× DIV pigs using the Porcine  
358 SNP60 BeadChip (Illumina). DIV was a synthetic line derived by crossing Landrace, Large  
359 White, Tongcheng or Meishan pigs.

## 1

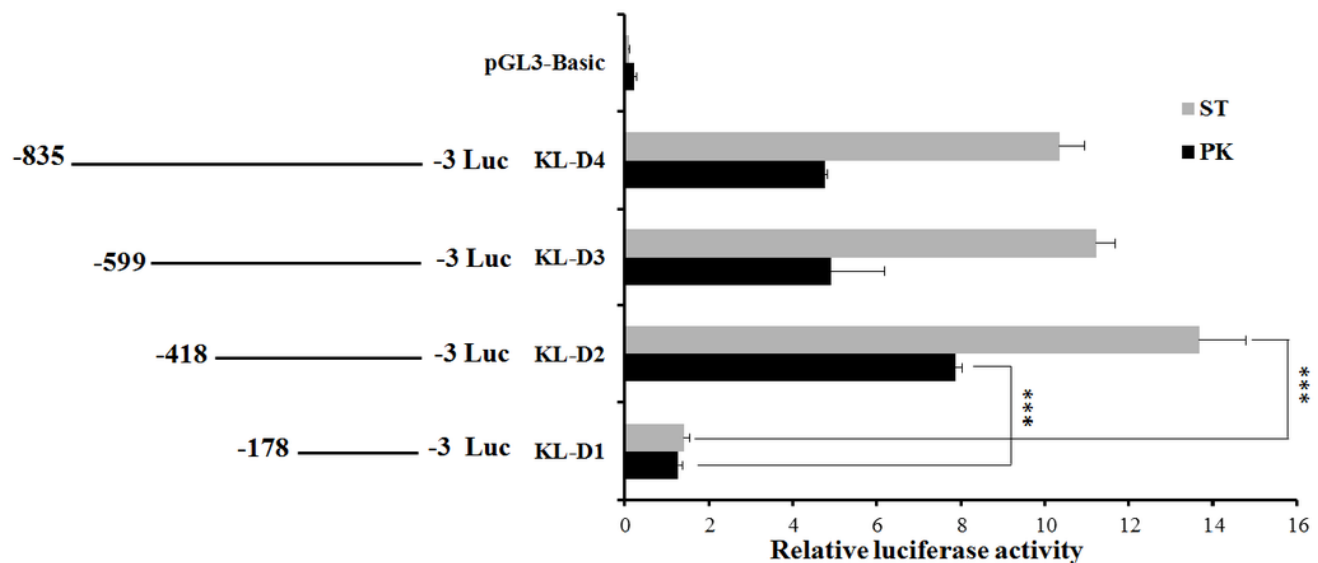
Deletion analysis of pig *KL* promoter.

(A) Schematic diagram of *KL* promoter, MARC0022311 (*KL* g.1474 A>G) and OCT-1 binding site in intron 1. (B) Promoter activities of a series of deleted constructs determined by luciferase assay. Left panel, relative location of four deletion fragments. The nucleotides were numbered from the potential transcriptional start site assigned as +1. Right panel, the relative luciferase activities of four reconstructed vector contained sequence from KL-D1 to KL-D4. \*\*\*  $P < 0.001$ .

A



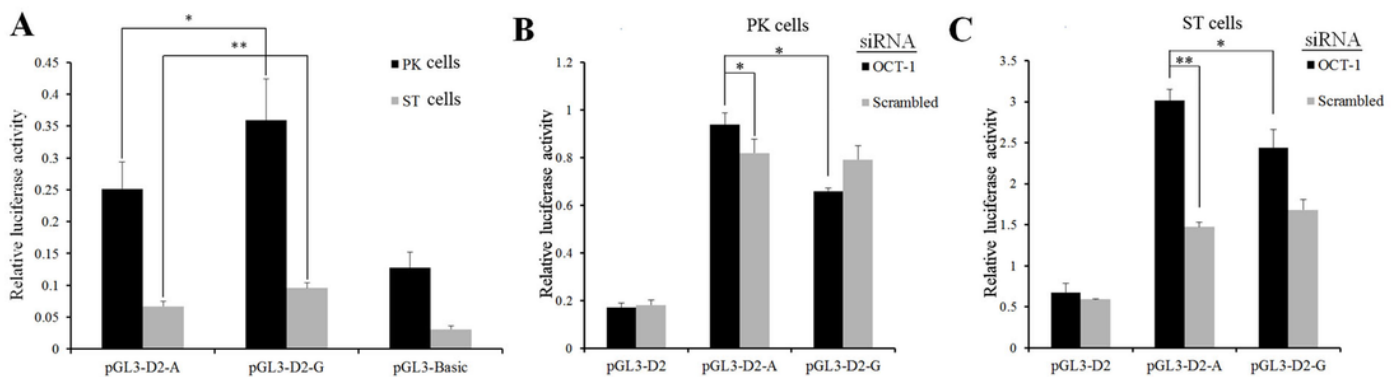
B



## 2

MARC0022311 in pig *KL* intron 1 affected promoter activity in PK and ST cells.

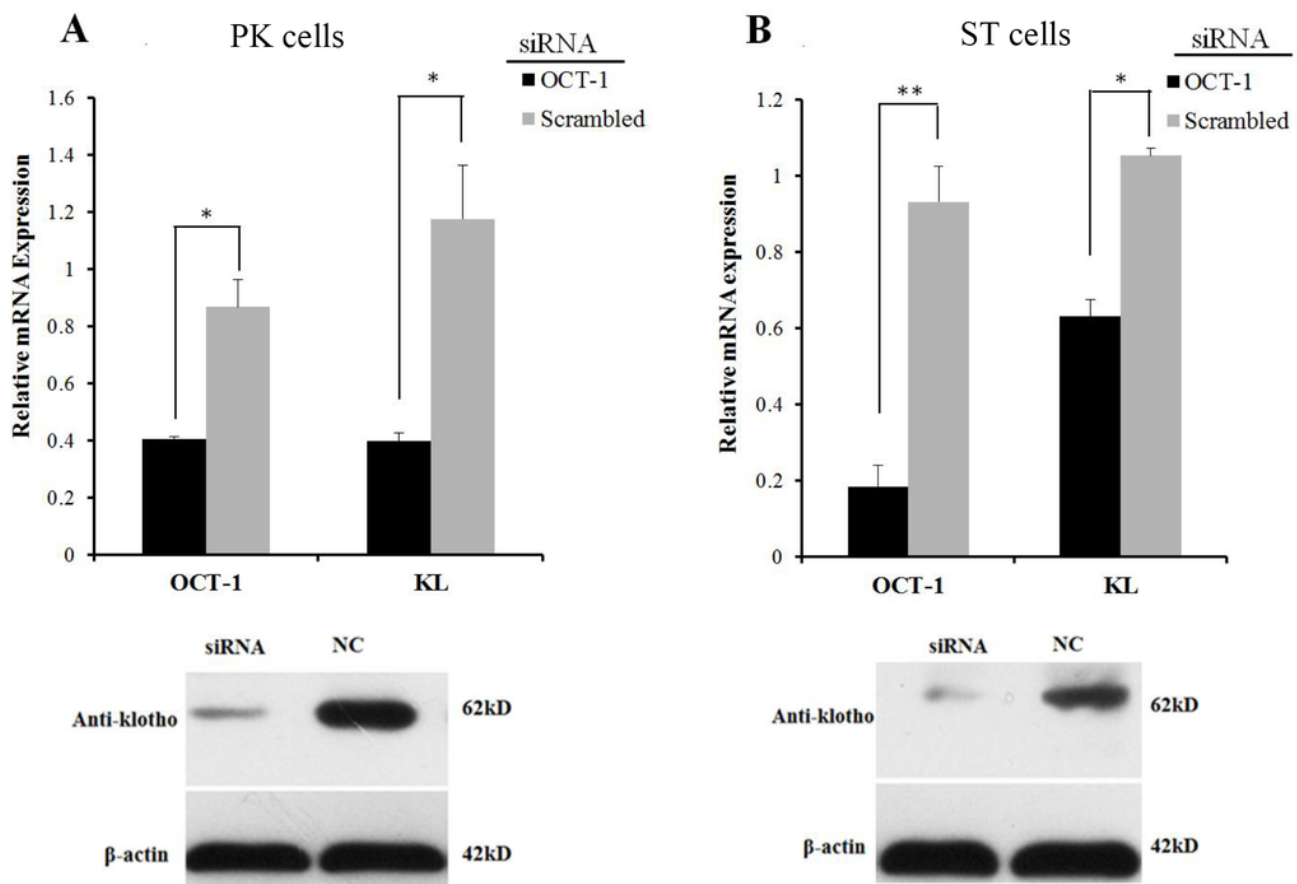
(A) Luciferase assays of reporter constructs using pig *KL*-D2 promoter and intron 1 fragments (g.1474 A and g.1474 G). (B) Luciferase detection after co-transfection of *OCT-1* siRNA with *pGL3-D2-A* and *pGL3-D2-G* in PK cells. (C) Luciferase detection after co-transfection of *OCT-1* siRNA with *pGL3-D2-A* and *pGL3-D2-G* in ST cells. \*  $P < 0.05$ . \*\*  $P < 0.01$ .



## 3

OCT-1 up-regulated *KL* expression by RNAi.

(A) PK cells were treated with 2  $\mu$ l *OCT-1* siRNA and 2  $\mu$ l NC for 24 h. Knockdown of *OCT-1* was confirmed by qPCR. *KL* mRNA and protein expressions were analyzed by qPCR and Western blotting. (B) ST cells were treated with 2  $\mu$ l *OCT-1* siRNA and 2  $\mu$ l NC for 24 h. Knockdown of *OCT-1* was confirmed by qPCR analysis. *KL* mRNA and protein expressions were analyzed by qPCR and Western blotting. \*  $P < 0.05$ . \*\*  $P < 0.01$ .



## 4

Binding of OCT-1 with *KL* intron 1 was analyzed by EMSA and ChIP.

(A) The probe was incubated with nuclear extract in the absence or presence of 100-fold excess of various competitor probes (mutant or non-labeled probe) or anti-OCT-1. The specific super-shift (DNA-protein-antibody complex) bands were both observed in PK and ST cells. The sequences of various probes were demonstrated under the panel. (B) ChIP assay of OCT-1 binding to the *KL* intron 1 in PK cells and ST cells. The interaction of OCT-1 *in vivo* with *KL* intron region was determined by chromatin immunoprecipitation analysis. DNA isolated from immune-precipitated material was amplified by PCR to amplify *KL* fragment. Total chromatin was used as the input. Normal mouse IgG was used as a negative control.

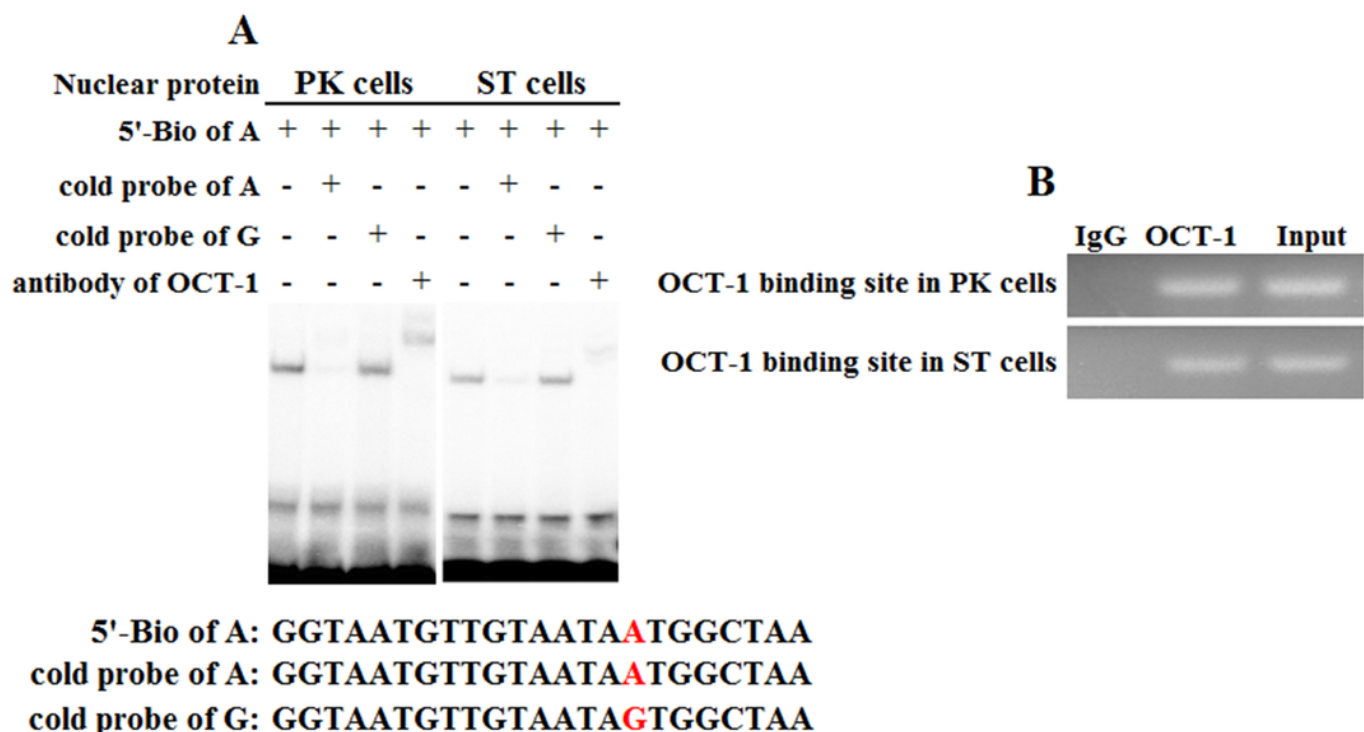


**Table 1** (on next page)

Primers and DNA oligos used in this study.

1 **Table 1. Primers and DNA oligos used in this study.**

Primer	Primer sequence (5'-3')	Amplicon Length (bp)	T <sub>m</sub> (°C)
5'-Bio of A (+)	GGTAATGTTGTAATAATGGCTAA		60
5'-Bio of A (-)	TTAGCCATTATTACAACATTACC		
cold probe of A (+)	GGTAATGTTGTAATAATGGCTAA		60
cold probe of A (-)	TTAGCCATTATTACAACATTACC		
cold probe of G (+)	GGTAATGTTGTAATAGTGGCTAA		60
cold probe of G (-)	TTAGCCACTATTACAACATTACC		
<i>KL_ChIP_PF</i>	TGAAGACCACTGCTACACACTT		59
<i>KL_ChIP_PR</i>	AGCAAACAGGTTTTGTGGAGC		
	<b>CGGGGTACCTTGTGGATGTTTTGTT</b>		
<i>KL_D1_PF</i>	TGTCTAGCTAGC	193	58
<i>KL_D_PR</i>	<b>CGACGCGTCCCTGTGAAGGCTTGTTT</b>		
	<b>CGGGGTACCTATGAGGAGGTGGGTT</b>		
<i>KL_D2_PF</i>	GGCTAGCTAGC	433	59
<i>KL_D_PR</i>	<b>CGACGCGTCCCTGTGAAGGCTTGTTT</b>		
	<b>CGGGGTACCCACTTAACCTCTTATTC</b>		
<i>KL_D3_PF</i>	TTGAGTTACTAGCTAGC	614	59
<i>KL_D_PR</i>	<b>CGACGCGTCCCTGTGAAGGCTTGTTT</b>		
	<b>CGGGGTACCACATAAAAGTTAGAAA</b>		
<i>KL_D4_PF</i>	ATCAGAGAACTAGCTAGC	850	59
<i>KL_D_PR</i>	<b>CGACGCGTCCCTGTGAAGGCTTGTTT</b>		
<i>OCT1_qPCR_PF</i>	TGAACAATCCGTCAGAAACC	196	58
<i>OCT1_qPCR_PR</i>	TGAGCAGCAGCCTGTAAACT		
<i>KL_qPCR_PF</i>	ACCCGTATTTATTGATGGAGAC	173	57
<i>KL_qPCR_PR</i>	GGAACCTTCATCTGAGGGTCTAA		
<i>KL_intron1_ChIP_PF</i>	GCCGTAGATAATTGAAGC	130	50
<i>KL_intron1_ChIP_PR</i>	TCTGTGGTAGCAAACAGG		
<i>KL_intron2_ChIP_PF</i>	GCCAGTGTAAGGTGTTACC	114	51
<i>KL_intron2_ChIP_PR</i>	ATTCTCCAAAGAAGACATACA		
<i>KL_intron3_ChIP_PF</i>	CAAGATTGTACCGTGGAG	171	50
<i>KL_intron3_ChIP_PR</i>	GGTCATTTGACATCATTCT		

2 Protective bases and induced enzyme sites were in italic and bold respectively.

3